Band structure of spin-Peierls cuprate CuGeO$_3$

Band structure of spin–Peierls cuprate CuGeO₃

Zoran S Popović, Filip R Vukajlović and Željko V Šljivančanin

Laboratory for Theoretical Physics and Physics of Condensed Matter (020), Institute of Nuclear Sciences—'Vinča', PO Box 522, 11001 Belgrade, Yugoslavia

Abstract. The spin-restricted and spin-polarized fully self-consistent linear muffin tin orbital band calculations for cuprate CuGeO₃ are presented with Cu atoms in normal and displaced positions within the orthorhombic cell. This, computationally much cheaper, approach gives practically the same one-electron bands as recent linear augmented plane wave calculations, and the same qualitative explanation for the spin–Peierls transition observed at low temperatures in this compound. New self-consistent spin-polarized calculations of CuGeO₃, for some supposed antiferromagnetic order in copper chains along the orthorhombic c axis, have given very small values for magnetic moments on Cu atoms. Again the dimerization of CuO₂ chains can open a band gap at E_F, if the Cu displacements in neighbouring chains are out of phase.

1. Introduction

The discovery that the cuprate CuGeO₃ is the first inorganic compound, containing linear spin-$\frac{1}{2}$ CuO₂ chains along the orthorhombic c axis, exhibiting a spin–Peierls (SP) transition [1], has led to intensive experimental investigations of various physical properties of this material [2–7]. The spin–Peierls is a kind of magnetoelastic transition occuring in a system of linear Heisenberg antiferromagnetic (AF) chains, when this system undergoes transformation to dimerized or alternating AF linear chains. The spin–Peierls transition had been previously discovered only in organic compounds [8].

Several facts unambiguously showed the occurrence of a spin–Peierls transition in CuGeO₃. Specifically, [1, 3, 4] and [9] presented the investigations of the temperature dependence of the magnetic susceptibility, which shows an abrupt decrease near 14 K. That fact has been interpreted [1, 3, 4] as a phase transition from a uniform AF spin-$\frac{1}{2}$ Heisenberg chain to a system of dimerized chains with a singlet ground state and ∼24 K energy gap. Neutron and x-ray measurements [4] show a second-order phase transition at $T = 14$ K while the magnetic field dependence of the structural transition temperature [1] confirms the spin–Peierls interpretation and excludes the possibility of a pure structural transition. Experimental results of the temperature dependence of the susceptibility of the crystalline CuGeO₃ of [9] are very similar to the results of [1], except for the existence of a sharp rise for $T < 7$ K and a larger and different anisotropy of the susceptibility. The authors claimed that the magnetic long-range order (Néel order) exists in the CuGeO₃ system below 7 K and did not attribute the sharp drop of the susceptibility to any kind of phase transition.

In contrast to relatively detailed experimental investigations of CuGeO₃, the only theoretical work devoted to the system of this type appeared only recently [10], in an attempt to investigate the applicability of standard band methods and the local density

approximation (LDA) [11]. A scalar relativistic version of the linear augmented plane wave (LAPW) method has been applied in order to calculate the non-magnetic band structure of orthorhombic $CuGeO_3$. Unusual transport properties, together with the dimerization of the CuO_2 chains along the orthorhombic c axis and the gap opening at the spin–Peierls transition could be predicted by Mattheiss, by means of a combined first-principles LAPW and linear combination of atomic orbitals (LCAO) tight-binding (TB) description of $CuGeO_3$. In order to explore the effect of a few selected distortions on the $CuGeO_3$ bands near E_F, a 15-parameter TB model has been set up, based on a fit to LAPW results in eight Brillouin zone (BZ) points (RMS error $\sim$0.5 eV). Mattheiss analysis favours a staggered pairing of Cu atoms along CuO_2 chains and predicts a basic structural feature of the low-temperature spin–Peierls distortion in this system.

Investigations of crystalline systems with a large number of atoms in the unit cell and a lot of empty space in the structure is hampered by the computational size due to a relatively large number of basis functions needed in the LAPW method.

Our aim in this paper is to investigate the electronic and magnetic structure of $CuGeO_3$ by use of another linear method, computationally much cheaper, i.e., the linear muffin tin orbital (LMTO) method [12, 13]. It is well known that the spin-independent electronic structures of the high-temperature copper oxide superconductors, another type of material with pronounced electronic correlation effects, are only weakly dependent on the particular choice of the computational scheme (e.g., linear augmented plane waves and linear muffin tin orbital), and exchange–correlation potential [14].

But, the relative ease of obtaining single-particle band structures of complex systems enables us to perform more complete, fully self-consistent, both spin-restricted and spin-polarized calculations of the cuprate $CuGeO_3$. In this work we have been interested in the possibility of gap opening at E_F when Cu atoms in neighbouring chains are displaced vertically ($\delta \approx 0.05$ Å) with opposite and the same phases. The feasibility of getting the insulating character of $CuGeO_3$ due to the specific antiferromagnetic ordering is also a problem which will be addressed here.

The layout of this paper is as follows. Firstly, in section 2, we describe the details of the calculation specific for this compound. In section 3 we present fully self-consistent paramagnetic and antiferromagnetic results for the normal and distorted orthorhombic unit cell. In the conclusion of the paper we discuss the agreement between some of our results and recent theoretical results [10] and the failure of the local spin density approximation (LSDA) to describe the experimentally observed effective magnetic moments in [9].

2. Details of the calculations

The self-consistent electronic structure calculations were done for $CuGeO_3$ in both non-magnetic and in several supposed antiferromagnetic states. The changes in electronic and magnetic structure, when Cu atoms in neighbouring chains are displaced vertically with the same and opposite phases, were also investigated. The bands were calculated using the spin-restricted and spin-polarized version of the LMTO method in the atomic sphere approximation (ASA) [12, 13]. The exchange–correlation potential used in our calculations is the von Barth–Hedin potential [15]. The initial charge densities were calculated using standard Hartree–Fock–Dirac programs with initial configuration core $+ 3d^{10}4s^1$ for copper, core $+ 4s^24p^2$ for germanium and core $+ 2s^22p^4$ for oxygen. A frozen core approximation was used; we iterated to self-consistency on valence electrons only.

In previous investigations of crystal structure there is some disagreement about the space group of cuprate $CuGeO_3$ (more precisely, copper metagermanate [7]). Namely, in

[2, 9, 16] it is stated the that space group is $Pb2_1m$ (C_{2v}^2), while in [1, 4, 7] and [17] it was shown that CuGeO₃ belongs to the *Pbmm* (D_{2h}^5) space group. Actually, the details of the low-temperature structure have not yet been determined precisely [10].
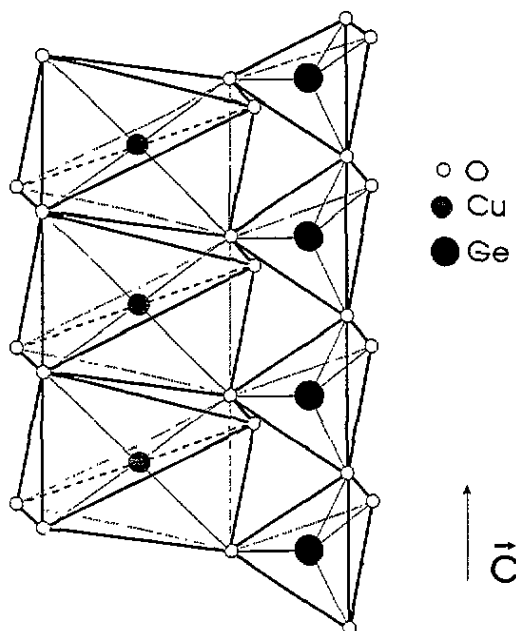

Figure 1. Spatial arrangement of atoms in CuGeO₃.

The room temperature crystal structure is orthorhombic *Pbmm* (D_{2h}^5) with two formula units per unit cell [17]. We will accept these structural results for our theoretical calculations in order to be able to compare them with the calculations of Mattheiss [10]. As shown in figure 1 the basic building blocks of the CuGeO₃ structure are strongly deformed CuO₆ octahedra connected through short common edges. These octahedra form edge sharing CuO₂ chains along the *c* axis, which are uniform above the spin–Peierls transition and become dimerized by distortion near 14 K. Beside these, there are corner sharing GeO₄ tetrahedra also forming *c* axis chains. The distance between Cu and O atoms in CuO₄ squares is 1.94 Å, while the distance between Cu and apical oxygens is ∼2.77 Å. The average distance between Ge and O is ∼ 1.74 Å and distances between oxygen atoms are from 2.54 to 2.95 Å.

Calculations for the orthorhombic structure of CuGeO₃ were carried out using the radii of the spheres around the atoms listed in table 1, including the six empty spheres (ES$_I$ − ES$_{III}$)₂. In this table and throughout this paper we denote apical oxygen in the deformed CuO₆ octahedra as O$_I$; the other oxygens are denoted as O$_{II}$. We have used 30 *k* points in the irreducible wedge of the Brillouin zone.

3. Results

3.1. Paramagnetic calculations

The electronic band structure of cuprate CuGeO₃ with 10 atoms and six empty spheres per unit cell (positions and sphere radii are given in table 1) have been calculated using the

Table 1. Atomic positions, types, and sphere sizes for LMTO calculation of orthorhombic $(CuGeO_ICaO_{II}O_{II}ES_IES_{II}ES_{III})_2$. Unit cell parameters are $a = 9.089585$ au, $b = 16.005985$ au, $c = 5.55768$ au, corresponding to 4.81, 8.47 and 2.941 Å, respectively. The x, y and z coordinates for the atomic positions are in units of a, b and c. ES_{I-III} signify different types of empty sphere.

No	Atom	Type	Atomic position			R
			$x(a)$	$y(b)$	$z(c)$	(au)
1	Cu	1	0.5	0.0	0.0	2.569027
2	Cu	1	0.5	0.5	0.0	2.569027
3	Ge	2	0.0743	0.25	0.5	2.401028
4	Ge	2	0.9257	0.75	0.5	2.401028
5	O_I	3	0.87	0.25	0.0	1.737827
6	O_I	3	0.13	0.75	0.0	1.737827
7	O_{II}	4	0.2813	0.0838	0.5	1.737827
8	O_{II}	4	0.7187	0.5838	0.5	1.737827
9	O_{II}	4	0.7187	0.9162	0.5	1.737827
10	O_{II}	4	0.2813	0.4162	0.5	1.737827
11	ES_I	5	0.57565	0.25	0.5	2.692194
12	ES_I	5	0.42435	0.75	0.5	2.692194
13	ES_{II}	6	0.0	0.0	0.0	2.861935
14	ES_{II}	6	0.0	0.5	0.0	2.861935
15	ES_{III}	7	0.29158	0.25	0.0	1.914812
16	ES_{III}	7	0.70842	0.75	0.0	1.914812

ordinary LMTO ASA [12, 13] method. The results for one-electron energy bands and density of states (DOS) are plotted in figures 2 and 3 respectively. When comparing calculated bands with those of earlier calculations, a consistency is found with those calculated on the basis of the LAPW by Mattheiss [10]. The small differences between the present values for one-electron energies and those of [10] is not surprising, since the computational methods are quite different.

The 28 lowest-lying valence bands are predominantly of O 2p and Cu 3d character, as could be seen from the projected density of states (figure 3). The first pair of unoccupied bands is mainly formed of Ge 4s, 4p states. The same two nearly degenerate half-filled quite narrow (~ 1 eV) conduction bands which are crossed by the Fermi level are also evident in figure 2. These bands are split off in energy from the fully occupied valence manifold, and this is a characteristic feature of cuprate $CuGeO_3$, which exhibits the spin–Peierls transition.

The total density of states and projected density of states contributions within the individual muffin tin spheres, presented in figure 3, are practically indistinguishable from Mattheiss's figure 5.

Starting up the LMTO calculations in complex compounds is not easy. In order to save time and eliminate the appearance of the ghost bands in the initial stages of the LMTO calculations, we give the self-consistent paramagnetic potential parameters (table 2).

Proceeding further we tried to explain recently reported neutron diffraction experiments [3], that predict out of phase dimerization along the two Cu chains in the cell. Using the advantage of the LMTO ASA over expensive full-potential LAPW calculations, we did fully self-consistent calculations with in- and out-of-phase Cu displacement in neighbouring chains. Since these displacements destroy the translational periodicity along the c axis, it was necessary to double the cell in this direction (20 atoms and 12 empty spheres). Like Mattheiss [10], vertical displacements of Cu atoms of 0.05 Å have been chosen. Our results
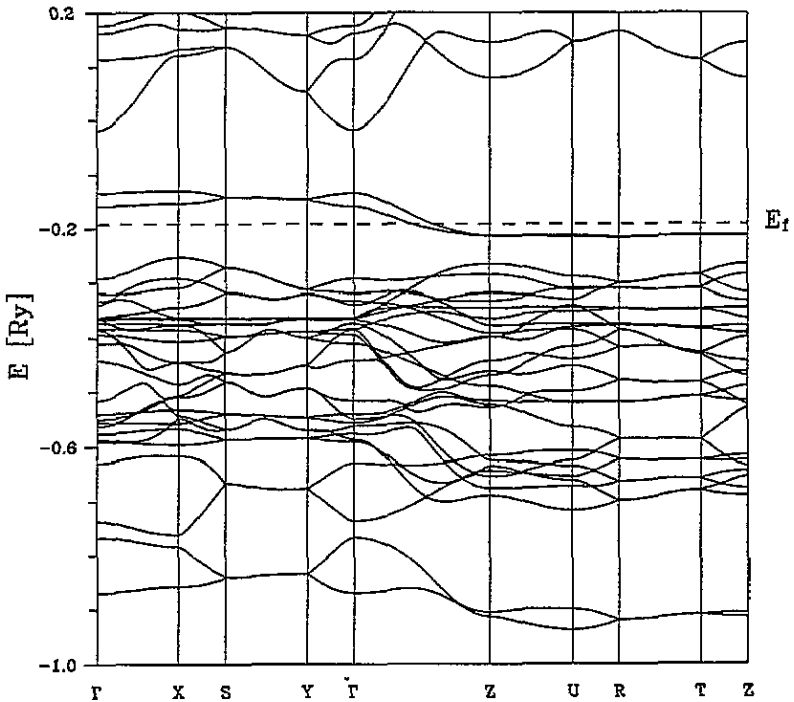
Figure 2. LMTO ASA energy band results for CuGeO₃ along several BZ directions. ΓXSYT and ZURTZ directions are perpendicular and ΓZ is parallel to the linear chain axis.

for the most interesting bands in the vicinity of the Fermi level are presented in figure 4.

Our self-consistent results support Mattheiss's conclusions based on a 15-parameter TB model fit to LAPW results at eight BZ points (figure 6 in [10]), e.g., a small gap at E_F is opened when Cu atoms in neighbouring chains are displaced vertically with opposite phases (figure 4(a)), while no gap opening occurs by in-phase distortion (figure 4(b)).

According to our results the out-of-phase displacements produce a state which has lower energy than the state with in-phase displacements of the same magnitude (figure 4(b)), or the initial undistorted state. This fact could be taken only as a qualitative support of a basic structural feature of the low-temperature spin–Peierls distortion in cuprate CuGeO₃, i.e., that the staggered pairing of Cu atoms along neighbouring CuO₂ chains should be expected. Insufficient accuracy of LMTO ASA total-energy calculations, based on the spherical charge density, make the obtained total energy lowering per atom comparable to the well known LMTO ASA error of the order of $\sim 10^{-2}$ Ryd.

4. Antiferromagnetic calculations

It is well known that three-dimensional magnetic effects are always present to some extent, if non-magnetic ions separate the copper chains [18]. Bearing in mind the experimental results of Petrakovski *et al* [9], where antiferromagnetic long-range order in CuGeO₃ was reported, it looked sensible to us to check this fact theoretically. We additionally did completely new and extensive, self-consistent spin-polarized LMTO ASA investigations of some of the supposed antiferromagnetic states with regular and distorted Cu chains. Three different spin-polarized calculations were performed: (a) first with an undistorted doubled
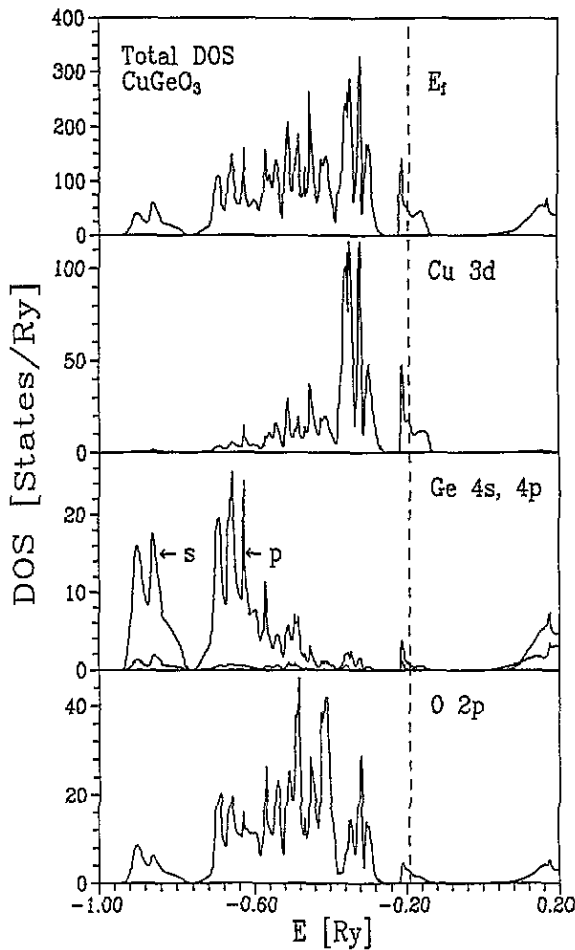
Figure 3. Total and partial self-consistent density of states results for CuGeO$_3$.

cell with antiferromagnetic ordering on Cu atoms along the c axis; (b) second for dimerized spin singlet chains with out-of-phase displacements in neighbouring CuO$_2$ chains and (c) third for in-phase displacements in neighbouring chains.

The one-electron energies and the density of states for the above-mentioned cases (a), (b) and (c) are almost identical with corresponding paramagnetic results. Because of that we have decided to give more details only for the case (b) (table 3 and figure 5). The self-consistent magnetic moments on Cu atoms 0.16, 0.13 and 0.14μ_B were obtained for the undistorted, out-of-phase and in-phase-distorted CuO$_2$ chains along the c axis. We obtained again that the antiferromagnetic state with antiparallel distortion of CuO$_2$ chains has the lowest energy. In addition to this, all spin-polarized results have greater LMTO ASA total energies than respective spin-restricted calculations, supporting the spin–Peierls transition in this compound. Again, these total-energy results should be taken only qualitatively. On the other hand, very poor agreement with effective experimental magnetic moments at copper sites (2.19μ_B for polycrystalline and 0.7μ_B for amorphous samples [9]) could be assumed as a manifestation of the well known local spin density approximation failure to account properly for electronic correlations in copper oxides.

Table 2. Standard self-consistent potential parameters obtained in spin-restricted calculations, as defined in [13].

L	E_ν	$\omega(-)$	$S\phi^2(-)$	$\phi(-)/\phi(+)$	$\langle\dot\phi_\nu^2\rangle^{1/2}$
			Atomic number: 29		
Copper					
			ASA radius: 2.569 027		
0	−0.566 072	0.143 832	0.364 082	0.848 603	0.212 397
1	−0.536 088	1.200 753	0.350 835	0.684 269	0.148 069
2	−0.380 009	−0.000 847	0.019 748	−0.022 351	1.460 154
Germanium				Atomic number: 32	
			ASA radius: 2.401 028		
0	−0.829 595	−0.349 365	0.363 638	0.805 554	0.259 422
1	−0.613 585	0.626 744	0.324 520	0.616 372	0.177 940
2	2.000 000	−0.037 818	0.301 966	0.353 544	0.192 401
				Atomic number: 8	
Oxygen-I					
			ASA radius: 1.737 827		
0	−1.800 000	−0.150 128	0.421 761	0.759 187	0.237 149
1	−0.521 309	0.124 019	0.266 019	0.360 611	0.279 381
2	−0.652 308	5.610 782	0.774 819	0.590 771	0.052 351
				Atomic number: 8	
Oxygen-II					
			ASA radius: 1.737 827		
0	−1.800 000	−0.159 547	0.418 393	0.758 224	0.238 934
1	−0.513 749	0.102 156	0.262 831	0.356 178	0.282 847
2	−0.471 219	5.386 418	0.760 571	0.584 767	0.053 771
Empty sphere-I				Atomic number: 0	
			ASA radius: 2.692 194		
0	−0.573 033	0.532 926	0.328 866	0.852 820	0.257 356
1	−0.531 051	1.572 183	0.361 889	0.711 641	0.141 631
2	−0.505 098	3.173 097	0.413 054	0.648 114	0.088 138
				Atomic number: 0	
Empty sphere-II					
			ASA radius: 2.861 935		
0	−0.555 743	0.396 238	0.293 467	0.848 934	0.297 290
1	−0.505 495	1.287 167	0.318 160	0.705 945	0.163 908
2	−0.488 111	2.695 450	0.362 597	0.643 794	0.101 411
				Atomic number: 0	
Empty sphere-III					
			ASA radius: 1.914 812		
0	−0.631 922	0.702 679	0.588 528	0.836 312	0.154 009
1	−0.572 554	2.795 049	0.674 467	0.699 223	0.078 061
2	−0.557 435	6.022 287	0.789 864	0.641 343	0.046 606

5. Conclusions

The results of paramagnetic local density functional and local spin density functional LMTO ASA band structure calculations of orthorhombic CuGeO₃ have been presented. We have also investigated the influence of several possible distortions of Cu atoms in CuO₂ chains along the c axis on the electronic and magnetic structure. All results presented were obtained fully self-consistently. Like Mattheiss [10], our calculations have been performed simply with the intention of elucidating the overall bonding characteristics and the possibilities and limitations of band structure methods to treat the presently unique inorganic compound exhibiting a spin–Peierls transition.

Our calculations are similar to Mattheis [10], but differ from the latter in several important respects.

Firstly, we have used the LMTO method whereas he has used an LAPW description.
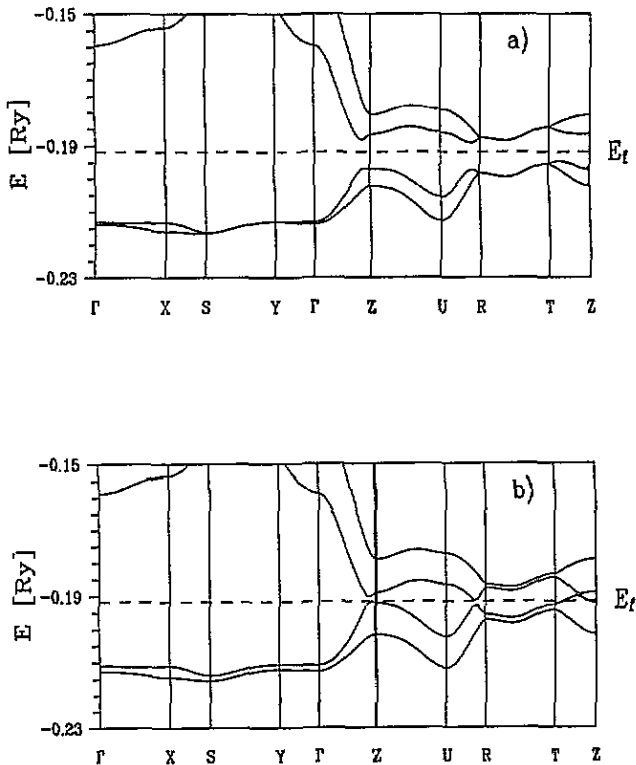
Figure 4. Self-consistent paramagnetic LMTO ASA energy bands near E_F for dimerized Cu atoms with vertical displacements in neighbouring CuO_2 chains that are either (a) antiparallel or (b) parallel.

Secondly, we have used the simple atomic sphere approximation, whereas he has used the more elaborate and time consuming full-potential LAPW method.

Thirdly, to explore the effect of a few selected distortions on $CuGeO_3$ bands near E_F, we did our investigations of a double cell with dimerized Cu atoms with vertical in- and out-of-phase displacements *ab initio* and fully self-consistently, while he used a 15-parameter tight-binding model, based on a fit to LAPW results at eight Brillouin zone points (RMS error ~0.5 eV).

Completely new, and fully self-consistent, spin-polarized LDA calculations of several supposed antiferromagnetic configurations in $CuGeO_3$, both with and without distortion in neighbouring Cu chains along the c axis, have been done also.

The following clear conclusions emerge from our calculations.

(A) In the part where we have been repeating exactly what Mattheiss did, spin-restricted LMTO ASA one-electron eigenvalues agree excellently with the LAPW full-potential results. DOS curves are practically indistinguishable (figure 5 in [10] and figure 3 in this work). Contrary to the experiment, this spin-restricted picture predicts metallic behaviour in $CuGeO_3$. Both calculations predict the presence of two nearly degenerate half-filled conduction bands with surprisingly narrow (~1 eV) width. Mattheiss [10] has demonstrated that this σ^* band, despite its visual simplicity, should be described within a sufficiently complex tight-binding five-band model.

(B) *Ab initio* and self-consistent LMTO ASA calculation of the doubled $CuGeO_3$ cell
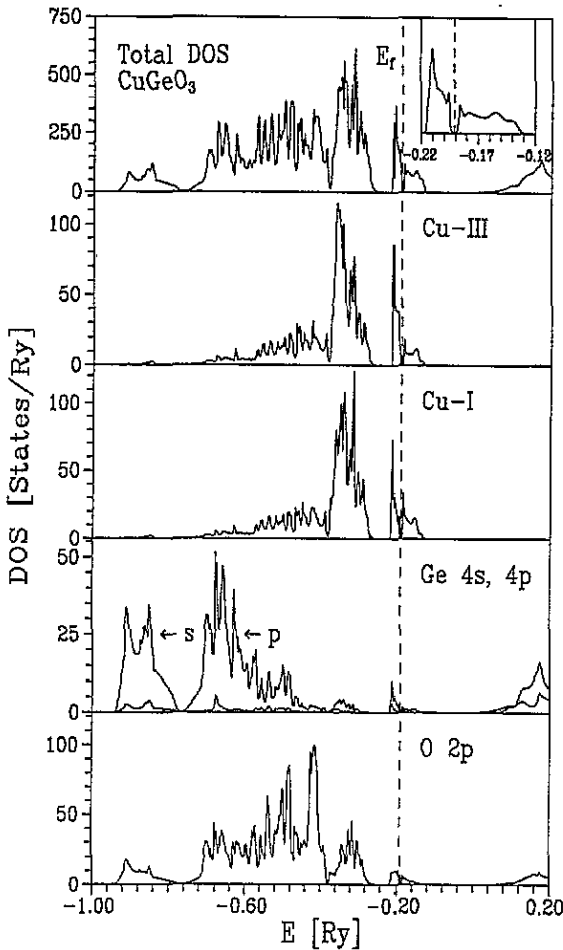
Figure 5. Total and partial self-consistent density of states of $CuGeO_3$, for antiferromagnetically ordered, out-of-phase distorted, Cu atoms in CuO_2 chains along the c axis. Inset gives enlarged region around the energy gap.

supports Mattheiss's [10] tight-binding result that, at the spin–Peierls transition, the dimerization of the CuO_2 chains can open a band gap at E_F, provided that the Cu displacements in the neighbouring chains are out of phase.

(C) Spin-polarized LMTO ASA calculations of cuprate $CuGeO_3$, for the supposed antiferromagnetic order in copper chains along the c axis, have given very small magnetic moments and minor changes in one-electron energy bands. The introduction of a magnetic moment of the opposite sign at Cu sites in the doubled orthorhombic cell does produce a splitting of the folded version of the bands at every point in k space. The magnitude of the calculated splitting of the undistorted lattice is ~0.15 eV, too small relative to the bandwidths (~1.2 eV), to open a gap at Fermi level. The calculated moments at Cu sites are $0.16\mu_B$ and are too small compared to the above-mentioned experimental results [9]. Out-of-phase Cu displacements in neighbouring chains of the doubled unit cell gave again the gap at the Fermi level (~0.1 eV) and a magnetic moment of $0.13\mu_B$ per Cu atom along the c axis. All spin-polarized results have greater LMTO ASA total energy than respective spin-restricted calculations, thus supporting qualitatively the spin–Peierls explanation of

Table 3. Data from self-consistent LSDA band structure calculation for antiferromagnetic CuGeO$_3$ and out-of-phase distortion along the c axis. Cu-I is the first copper atom in its original position, while Cu-III is the subsequent copper atom in the distorted position and with the antiparallel spin along the c axis.

	Orbital	Cu-I	Cu-III	Ge	O–I
	s$\uparrow$	0.229	0.230	0.367	0.059
	s$\downarrow$	0.229	0.229	0.367	0.059
Occupation per spin	p$\uparrow$	0.281	0.282	0.624	1.832
per atom	p$\downarrow$	0.281	0.282	0.624	1.832
	d$\uparrow$	4.632	4.767	0.258	0.001
	d$\downarrow$	4.765	4.634	0.258	0.001
	Total $\uparrow$	5.142	5.279	1.249	1.892
	Total $\downarrow$	5.275	5.145	1.249	1.892
Contribution to	s	0.000	−0.001	0.000	0.000
magnetic moment	p	0.000	0.000	0.000	0.000
per atom	d	0.133	−0.133	0.000	0.000
	s$\uparrow$	−0.419	−0.424	−1.177	−1.950
	s$\downarrow$	−0.424	−0.419	−1.177	−1.950
Band centres	p$\uparrow$	0.632	0.626	0.004	−0.397
(Ryd)	p$\downarrow$	0.632	0.632	0.004	−0.397
	d$\uparrow$	−0.374	−0.385	1.961	4.513
	d$\downarrow$	−0.385	−0.374	1.961	4.513

the observed transition in this compound, where the observed isotropic susceptibility below $T_c \sim 14$ K, in most of the experiments [1, 3, 4], excludes the possibility of antiferromagnetic long-range order in this system [19]. Bearing in mind the well known failure of the LSDA to describe electronic and magnetic properties of high-temperature superconducting parent compounds and other charge transfer insulators [14], the present failure of the LDA and LSDA to give better quantitative results should be taken as an indication of the importance of the electron correlations in the CuGeO$_3$ system.

But, single crystals of CuGeO$_3$ are translucent blue in colour, and transport measurement shows that these samples exibit insulating behaviour with room-temperature resistivity as high as $\rho(T = 300K) \approx 10^{13}$ Ω cm [10]. Most of the experiments support the spin–Peierls picture for the description of the electronic properties of CuGeO$_3$. This compound is presently the unique inorganic compound which exhibits a spin–Peierls transition and it will probably be a matter of interest for theoretical investigations in the near future. Our calculations suggest that the LMTO ASA should be used for both spin-restricted and spin-polarized calculations due to the computational speed and simplicity. A more careful treatment of the interactions beyond the LDA and LSDA is required to obtain an appropriate quantitative description of this system. The LMTO ASA enables one to incorporate easily some electron correlation effects behind the second Hund rule which are responsible for orbital polarization (ordering) and formation of local (atom-like) moments. Recently suggested so-called LDA+U method was very successfull in describing magnetism in copper oxides [20, 21] and we expect similar improvement in the case of CuGeO$_3$.

To support our suggestion for the LMTO ASA application, and as a matter of curiosity, we mention that all present extensive calculations were performed on an ordinary 66 MHz PC-486 with 16 MB of extended memory.

Acknowledgments

References

[1] Hase M, Terasaki I and Uchinokura K 1993 *Phys. Rev. Lett.* **70** 3651
[2] Sugai S 1993 *J. Phys. Soc. Japan* **62** 3289
[3] Nishi M 1994 *J. Phys.: Condens. Matter* **6** L19
[4] Pouget J P, Regnault L P, Ain M, Hennion B, Renard J P, Veillet P, Dhalenne G and Revcolevschi A 1994 *Phys. Rev. Lett.* **72** 4037
[5] Lorenzo J E, Hirota K, Shirane G, Tranguada J M, Hase M, Uchinokura K, Kojima H, Tanaka I and Shibuya Y 1994 *Phys. Rev.* B **50** 1278
[6] Hirota K, Cox D E, Lorenzo J E, Shirane G, Tranguada J M, Hase M, Uchinokura K, Kojima H, Shibuya Y and Tanaka I 1994 *Phys. Rev. Lett.* **73** 736
[7] Dević S D, Konstantinović M J, Popović Z V, Dhalenne G and Revcolevschi A 1994 *J. Phys.: Condens. Matter* **6** L745
[8] Bray J W *et al* 1975 *Phys. Rev. Lett.* **35** 774
   Jacobs I S *et al* 1976 *Phys. Rev.* B **14** 3036
[9] Petrakovski G A, Sablina K A, Vorotynov A M, Kruglik A I, Klimenko A G, Balayev A D and Aplesnin S S 1990 *Zh. Eksp. Teor. Fiz.* **98** 1382 (Engl. Transl. 1990 *Sov. Phys.–JETP* **71** 772)
[10] Mattheiss L F 1994 *Phys. Rev.* B **49** 14 050
[11] Hohenberg P and Kohn W 1964 *Phys. Rev.* **136** B864
   Kohn W and Sham L J 1965 *Phys. Rev.* **140** A1133
[12] Andersen O K 1975 *Phys. Rev.* B **12** 3060
[13] Skriver H L 1984 *The LMTO Method* (New York: Springer)
[14] For recent reviews, see
   Hass K C in 1989 *Solid State Physics* vol 42, ed H Ehrenreich, D Turnbull and F Seitz (New York: Academic) p 213 and references [32–43] therein
[15] von Barth U and Hedin L 1972 *J. Phys. C: Solid State Phys.* **5** 1629
[16] Ginetti Y 1954 *Bull. Soc. Chem. Belg.* **63** 209
[17] Völlenkle H, Wittmann A and Nowotny H 1967 *Monatsh Chem.* **98** 1352
[18] Steiner M, Villain J and Windsor C G 1976 *Adv. Phys.* **25** 87
[19] Buzdin A I and Bulaevskii L N 1980 *Uzp. Fiz. Nauk* **131** 495
[20] Anisimov V I, Zaanen J and Andersen O 1991 *Phys. Rev.* B **44** 943
   Anisimov V I, Korotin M A, Zaanen J and Andersen O K 1992 *Phys. Rev. Lett.* **68** 345
[21] Czyzyk M T and Sawatzky G A 1994 *Phys. Rev.* B **49** 12 211